Large-Scale Testing of Effects of Anti-Foam Agent on Gas Holdup in Process Vessels in the Hanford Waste Treatment Plant - 8280

LA Mahoney, JM Alzheimer, ST Arm, CE Guzman-Leong, LK Jagoda, CW Stewart,
BE Wells, and ST Yokuda
Pacific Northwest National Laboratory
P.O. Box 999, Richland, WA 99354

ABSTRACT

The Hanford Waste Treatment and Immobilization Plant (WTP) will vitrify the radioactive wastes stored in underground tanks. These wastes generate and retain hydrogen and other flammable gases that create safety concerns for the vitrification process tanks in the WTP. An anti-foam agent (AFA) will be added to the WTP process streams. Previous testing in a bubble column and a small-scale impeller-mixed vessel indicated that gas holdup in a high-level waste chemical simulant with AFA was as much as 10 times higher than in clay simulant without AFA. This raised a concern that major modifications to the WTP design or qualification of an alternative AFA might be required to satisfy plant safety criteria. However, because the mixing and gas generation mechanisms in the small-scale tests differed from those expected in WTP process vessels, additional tests were performed in a large-scale prototypic mixing system with in situ gas generation.

This paper presents the results of this test program. The tests were conducted at Pacific Northwest National Laboratory in a 1/4-scale model of the lag storage process vessel using pulse jet mixers and air spargers. Holdup and release of gas bubbles generated by hydrogen peroxide decomposition were evaluated in waste simulants containing an AFA over a range of Bingham yield stresses and gas generation rates. Results from the 1/4-scale test stand showed that, contrary to the small-scale impeller-mixed tests, holdup in the chemical waste simulant with AFA was not so greatly increased compared to gas holdup in clay without AFA. The test stand, simulants, scaling and data-analysis methods, and results are described in relation to previous tests and anticipated WTP operating conditions.

INTRODUCTION

The Hanford Waste Treatment and Immobilization Plant (WTP) will pretreat and vitrify a large part of the radioactive waste now stored in Hanford's underground storage tanks. Some of the WTP process streams are thick slurries with a relatively high solids fraction that are expected to exhibit non-Newtonian rheological behavior. Based on studies of pretreated tank waste samples, the Bingham model, using a yield stress, τ_y, and consistency factor, κ, adequately represents these non-Newtonian waste streams [1]. The WTP is being designed to process slurries with Bingham yield stress up to 30 Pa.

These fluids also generate flammable gases by a complex combination of radioactivity and chemical reactions [2] and, unless under shear, retain gas bubbles by their inherent strength. Therefore, the WTP process tanks must be mixed sufficiently well and often to prevent hazardous volumes of flammable gases from accumulating. Pulse jet mixers (PJMs) are the primary method of mixing most vessels in the WTP because they have no moving parts. A PJM consists of a large vertical pulse tube with an air pressure/ vacuum source connected to the top and a nozzle at the base exiting near the tank bottom. A WTP process tank may have 4, 8, or more pulse tubes with a total volume on the order of 10% of the total tank volume. PJMs operate by expelling slurry out through the nozzles at high velocity, after which a vacuum is applied to refill them with slurry.

Because PJMs had not been used in non-Newtonian slurries, an integrated scaled testing program was required to provide a technical basis for those WTP vessels expected to process them [3]. This program at Pacific Northwest National Laboratory resulted in a scaling theory for PJM mixing of non-Newtonian fluids [4] based on the concept of intermittent mixing within the PJM "cavern," a region near the PJM nozzles where the mobilized slurry experiences turbulent flow. Because the PJMs alone could not mix the region above the cavern without excessive compressed-air consumption, they were supplemented with air spargers.

The full-scale air-sparging systems consist of 15 to 36 pipes, 2 inches in diameter, that exit near the tank bottom. Each tube conducts 7 to 25 acfm of air, producing large bubbles that produce mixing action in a high-speed upwelling region of bubbles (ROB) surrounded by a slow downward flow in the wider zone of influence (ZOI). Correlations were developed from testing results at nearly full scale to relate the ROB and ZOI diameters by each sparger to the sparging air flow rate [5]. Adequate mixing is provided if sparge tubes are arranged so there is adequate overlap of the individual sparging-induced mixing regions. The combined system of PJMs plus spargers is identified as the "hybrid" mixing system.

Tests were conducted with physical simulant (kaolin-bentonite) and a chemical simulant of radioactive waste to determine the extent of retention of in situ generated gas. The tests that were performed in scaled prototypic test stands employed only the clay simulant, for cost reasons. Other tests that were carried out in a small-scale bubble column and a small-scale agitator-mixed test vessel used the clay, the chemical simulant without an anti-foaming agent (AFA), and the chemical simulant with an AFA. The latter test results seemed to show that AFA might produce or contribute to problematic levels of in situ gas retention [6]. However, the non-prototypic nature of the test equipment suggested that the AFA results might not be applicable in WTP operations. To resolve this issue and provide the necessary data on the effect of AFA on gas holdup, tests in clay and chemical simulant with and without AFA were recommended to be performed in a large-scale prototype PJM/hybrid-mixed vessel. The results of these tests, which differ from those of the non-prototypic systems, are described in this paper.

BACKGROUND

Slurry with a yield stress of 30 Pa is expected to retain bubbles up to about 5 mm equivalent diameter when not being mixed [7]. Therefore, the flammable gas bubbles retained in the WTP process slurry are small and distinct from the large sparged bubbles that rise rapidly to the surface whether or not the slurry is being mixed by PJMs. Gas is released from the slurry by the simple mechanism of bubbles rising through the slurry to the surface, where they eventually burst and release their gas to the atmosphere. Because mass conservation dictates that the average vertical velocity of the non-gas portion of the slurry is zero, the gas release rate is determined only by the relative rise speed of the bubbles relative to the slurry. The complexity and intensity of the slurry circulation is immaterial.

Mixing is neither uniform nor continuous in the PJM hybrid systems planned for the WTP. The PJM jets mix the slurry for only 30 seconds every few minutes. Spargers may not operate continuously. The intensity of mixing varies over the volume. However, an average or effective constant bubble rise speed, U_R, can be used to characterize the overall gas release performance of a specific mixing system. Under the assumption of constant rise speed, a mass balance on the in situ generated bubbles gives the following expression for the retained gas volume fraction, $\alpha(t)$ [8]:

$$\alpha(t) = \alpha_0 e^{-\frac{U_R}{H}t} + g_v \frac{H}{U_R}\left(1 - e^{-\frac{U_R}{H}t}\right)$$

(Eq. 1)

where
α_0 = initial gas volume fraction (volume of gas/total volume of slurry + gas)
H = effective slurry depth (m); equals slurry volume divided by vessel cross-sectional surface area
g_v = volumetric gas generation rate (1/s), (volume of gas generated/unit volume of slurry/unit time).

The effect of mixing on gas retention and release is defined by a time constant, H/U_R, where U_R includes the combined effects of intermittency and nonuniformity. The higher the bubble rise speed or the lower the slurry depth, the faster the gas is released and the lower the retained gas volume fraction is. If mixing continues for a long time, Eq. (1) reduces to a steady-state form:

$$\alpha_{ss} = \frac{g_v H}{U_R} = \frac{U_s}{U_R} \qquad \text{(Eq. 2)}$$

The product, $g_v H$, is the superficial gas velocity, U_s, which is the measure of the volumetric rate of gas volume flow per unit area. The bubble rise speed is generally higher for larger bubbles and lower yield stress slurries. It has been quantified reasonably well for Newtonian fluids [9, 10] but not for non-Newtonian slurries, especially Bingham model slurries [11, 12]. However, data from steady-state gas holdup tests to date in Bingham non-Newtonian slurries being sheared or mixed by PJMs alone, air sparging alone, a rotary mixing vane, or the buoyant force of the bubbles themselves [5, 6, 8, 13] have shown that the volume fraction, α, of these bubbles in transit is related to the gas superficial velocity of the generated gas, U_s, by an expression of the form:

$$\alpha_{ss} = AU_s^B \qquad \text{(Eq. 3)}$$

where A and B are positive constants characteristic of the mixing system and slurry rheology. Combining Eq. (2) and (3) expresses the bubble rise speed as

$$U_R = \frac{1}{A}U_s^{1-B} = \frac{1}{A^{1/B}}\alpha^{\frac{1-B}{B}} \qquad \text{(Eq. 4)}$$

The bubble rise speed thus is not constant, as assumed in Eq. (1), but with B < 1, which is the usual case, increases with gas volume fraction. Eq. (4) also provides a good model for transient gas release, though the transient-release constants are somewhat different from steady-state values [6].

Because the constants in Eq. (3) and (4) are known to depend on slurry rheology, it is logical to assume that they may also be affected by the anti-foam agent (AFA) chosen for the WTP. This AFA is a surface-active agent consisting mostly of polydimethylsiloxane[1] and polypropylene glycol.[2] It not only reduces the surface tension but changes the characteristics of the liquid-gas interface. Besides reducing or preventing surface foam, it generally appears to reduce the bubble size by either enhancing breakup or reducing coalescence. A net reduction in bubble size would reduce the effective bubble rise speed, thereby increasing the gas holdup. The question is, how much?

Tests were conducted in a 15-cm-diameter bubble column in 2004 to investigate the effects of gas com-position and waste rheology on gas holdup in water, clay, and a chemical simulant of radioactive waste with and without the chosen AFA [8]. Adding AFA to the chemical simulant increased gas holdup by a

---

[1] Polydimethylsiloxane is the silicone polymer $(CH_3)_3SiO[SiO(CH_3)_2]_nSi(CH_3)_3$, the hydrophobic part of the AFA.
[2] Polypropylene glycol is the hydrocarbon polymer $C_3H_8O_2$, the hydrophilic part of the antifoam mixture.

factor of 7 to 10 compared to the same simulant without AFA, for gas superficial velocities in the range of 2 to 10 mm/s. Similar ratios were observed when comparing chemical simulant with AFA to clay simulant. These data, however, were controversial because the bubbles representing the retained gas also provided the mixing and the bubbles were generated at a ceramic diffuser at the base of the column, a process that might be much more strongly affected by AFA than the process of generating bubbles in situ.

Concerns about the applicability and high uncertainty of the bubble column data eventually led to a test program at Savannah River National Laboratory (SRNL) to quantify the effect of AFA more precisely. Tests were performed in 2006 in a 43-cm-diameter vessel mixed by rotary agitators using the same simulants as the bubble column tests, with superficial velocities in the range of 0.01 to 10 mm/s [6]. Results showed that the effect of AFA alone was to increase the observed holdup in the chemical simulant by a factor of 2 to 4. The observed ratio of holdup in chemical simulant with AFA to holdup in clay was as much as 9. Taking uncertainties into account, the ratio could have been as high as ~15 at 0.01 mm/s. Because the increase was greater at lower yield stress and lower superficial velocity, the ratios, when extrapolated to lower-strength simulants or the lower gas-generation rates characteristic of process conditions, could potentially be higher than the highest observed values.

Concerns were also expressed about the mixing system similar to those about the bubble column results. In addition, the relationship of gas holdup versus gas superficial velocity (Eq. 3) in the agitator-mixed vessel without AFA diverged from those of earlier tests in larger vessels with prototypic mixing systems. Though mixing by the agitator system was independent of the bubble source, its action was unlike that of the PJM-sparger hybrid system planned for the WTP.

TEST STAND DESCRIPTION

Gas retention and release tests were conducted in the 1/4-scale prototype of the WTP lag storage vessel. The test stand uses a hybrid mixing system consisting of 8 PJMs and 7 spargers built on the lag storage test stand used in 2004 [8]. The PJMs and spargers are shown in profile and plan views in Figure 1. Figure 2 is a photo of the PJM-sparger cluster assembly. The simulant level was adjusted just above the welded flange that appears as a white line above the top of the pulse tubes.

Scaling of PJM operation for mixing non-Newtonian slurries has been established through a comprehensive testing program from 2003 to 2005 [3]. The primary nondimensional group that directly affects the size of the PJM mixing cavern is the yield Reynolds number, Re_τ, defined as the ratio of the dynamic stress to the at-rest shear strength of the non-Newtonian slurry:

$$Re_\tau = \frac{\rho_s u_0^2}{\tau_s}$$

(Eq. 5)

where ρ_s is the slurry density (kg/m^3), u_0 is the peak average PJM jet velocity (m/s), and τ_s is the shear strength (Pa) of the slurry. The ratio of the height of the PJM mixing cavern to tank diameter is constant in a geometrically scaled system if the PJM jet velocity is held constant. This requires reducing the drive time in proportion to the scale factor to expel the scaled volume of slurry. This scaling is also applied to the total cycle time.

The current 1/4-scale lag storage test stand is actually 1:4.29 scale based on tank diameter. All of the components were appropriately scaled as constrained by standard pipe sizes. The pulse tubes were standard 12-inch schedule 40 stainless steel with an inside diameter (ID) of 12 inches instead of the 11.2 inches required for rigorous scaling. However, the length of the pulse tube was reduced to maintain the correct volume. The PJM nozzles were standard 1-inch schedule 40 stainless steel of 1.049 inch ID,

13% larger than the exactly scaled 0.93 inches. This reduces the PJM jet velocity to 78% of the correct value at the scaled drive time. Applying a reduced drive time provided up to ~87% of the scaled velocity. The PJM scaling parameters for full-scale and 1/4-scale WTP lag storage tank geometry, filled with a non-Newtonian slurry with a Bingham yield stress of 30 Pa, are shown in Table I. The full-scale WTP lag storage vessel, the perfectly scaled 1/4-scale, and the current 1/4-scale lag storage vessel are listed.
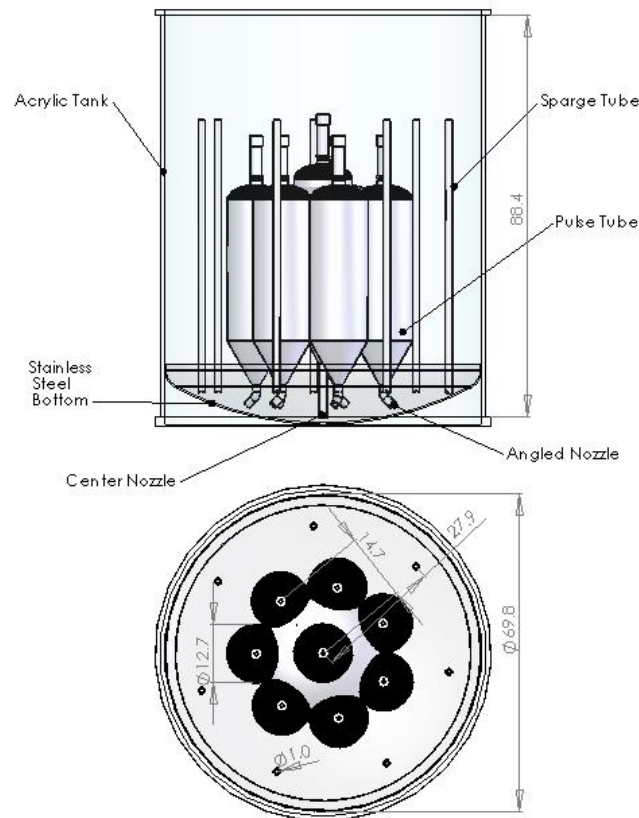

Fig. 1. 1/4-Scale PJM cluster and sparge tubes (units in inches).

Spargers cannot be scaled as precisely as PJMs. Rather than a relatively well-characterized jet, the active force in sparging is a population of poorly characterized, interacting bubbles, whose size, speed, and number are variable and do not depend on geometric scale ratios. Nevertheless, a measure of the power delivered to the slurry by rising bubbles can be derived in terms of hydrostatic pressure difference and flow rate. The total power per unit volume, P_V, generated by a steady population of bubbles rising through a slurry depth, H, can be expressed as

$$P_V = \frac{U_{sp}}{H} p_a \left(1 + \frac{\rho_s g H}{p_a}\right) \ln\left(1 + \frac{\rho_s g H}{p_a}\right) \qquad \text{(Eq. 6)}$$

where U_{sp} is the sparge gas superficial velocity and p_a is ambient atmospheric pressure at the surface. At a constant superficial velocity, P_V decreases slowly with reduced scale.

Fig. 2. Photograph of PJM and sparger assembly.

Table I. Scaled PJM Parameters for Lag Storage Vessels

Vessel	Scale Factor	Tank Diameter (in.)	Nozzle I.D. (in.)	Jet Velocity (m/s)	Re_τ	Drive Time (s)	Cycle Time (s)
Full scale	1	300	4	12	5,800	30	223
1/4-scale (exact)	4	75	1	12	5,800	7	56
1/4-scale (2007)	4.29	70	1.05	10.5	4,400	6	54

Because mixing effectiveness is related to power input, Eq. (6) suggests that similar sparger effectiveness can be maintained across scales with a constant superficial velocity of the air flow at the sparger tube exit (U_{sp} = 5.2 mm/s in the full-scale WTP design). Also, the current sparger design strategy is to overlap the up-flowing ROB from each of the spargers for uniform mixing. The following correlation of large-scale sparging test data [5] provides the ROB diameter in terms of the sparge actual volume flow rate, Q:

$$D_{ROB} = 3.78Q^{0.34} \qquad \text{(MKS units)} \tag{Eq. 7}$$

At a constant superficial velocity, the area fraction of the tank occupied by ROB varies more slowly than the scale factor, making the effect of sparging increasingly greater at smaller scale.

The full-scale tank uses 28 full-depth sparger tubes arranged in three concentric rings around the PJM cluster plus a number of partial-depth tubes above the PJMs. To compensate for over-sparging at the smaller scale and to reduce complexity, the 1/4-scale system uses 7 full-depth tubes in a single ring around the PJM cluster, as did the 1/2-scale lag storage test stand [13]. The sparge tubes are 1-inch ID PVC pipe with four 45-degree notches cut to a 3/8-inch depth in the end (Figure 2). This diameter makes the air exit velocity similar to the full-scale value at a constant superficial velocity. The

quantities derived above for the same test vessels presented in Table I are shown in Table II using a constant superficial velocity.

Table II. Scaled Sparger Parameters for Lag Storage Vessels

Vessel	Scale Factor	No. Spargers	Tube ID (in.)	Flow/tube (acfm)	A_{ROB}/A_T	Exit Velocity (m/s)	P_V (w/m^3)
Full scale	1.0	28	2	18	0.27	4.2	85
1/4-scale (exact)	4	28	0.5	1.1	0.65	4.2	69
1/4-scale (2007)	4.29	7	1	3.9	0.44	3.6	67

A large electric compressor supplied air at 125 psig at up to 400 acfm to a ~100 gallon surge tank immediately upstream of the air control manifolds. The control manifolds, each with its own pressure regulator and control valve, split into three streams: one supplies pressure to the PJMs, another provides PJM vacuum (via a venturi), and a third provides main sparger flow. A fourth air stream from the building air supply provided a continuous low "idle" sparge flow to keep simulant out of the spargers in the absence of the main air flow.

The PJM cycle consisted of drive, vacuum, static, and equilibration phases controlled by four valves operated automatically by the data acquisition and control system computer. Opening the drive valve allowed air to flow through the PJM manifold to the top of each pulse tube, expelling simulant through the nozzles at high velocity. During the vacuum phase, the drive valve closed and the vacuum valve opened, sending air through a venturi to pull a vacuum on the pulse tubes to quickly relieve the drive pressure, then apply a vacuum to refill the pulse tubes. During the static phase, the drive and vacuum valves closed and a downstream valve opened to the exhaust system to relieve the vacuum in the pulse tubes. During the equilibrium phase, the fourth valve was opened, connecting the tank dome space to the pulse tubes to bring the pressures and simulant levels to equilibrium. This phase provides a period relatively free from transient fluctuations and so is used for calculating the representative gas volume fractions from the recorded data, as described below.

TEST APPROACH

Hydrogen peroxide decomposition simulated the in situ gas generation occurring in the WTP.[3] In situ gas generation avoids the complications and potential bias of non-prototypic mechanical bubble generation (e.g., orifices, porous diffusers, mixing vanes). The maximum gas generation rate estimated in the full-scale WTP lag storage vessel[4] is equivalent to a superficial gas velocity of ~0.0004 mm/s. However, the 1/4-scale tests required superficial velocities of 0.025 to 0.1 mm/s to create measurable gas volume fractions in the range of ~0.5–1 vol%. This was achieved with flow rates of 33–130 mL/min of 31 wt% hydrogen peroxide solution. The hydrogen peroxide solution was introduced though 7 injection tubes exiting near each of the outer PJM nozzles that are visible in Figure 2.

Steady-state gas holdup tests were conducted as sequences of 3 increasing hydrogen peroxide injection rates, each held for 2 hours. Three sequences, each begun with a 2-hour mixing period without hydrogen peroxide injection, were performed for each simulant condition. Continuous sparging and PJM operation continued throughout this period. A gas release test that began by shutting down the PJMs and spargers to allow the residual hydrogen peroxide in the simulant to decompose and build up a retained gas inventory was performed at the end of the last test sequence. PJMs and spargers were re-started when gas

---

[3] This system represents lag storage vessels HLP-27A/B at 1:4.29 scale and the blend vessel, HLP-28, at 1:4.54.
[4] Derived from WTP calc. sheet 24590-WTP-M4C-V11T-00004 Rev. C, assuming the gas is 25% hydrogen.

ceased accumulating, as indicated by a return to nearly steady simulant surface level, initiating release. The release test stopped when the simulant surface level again reached near steady state.

Two different non-Newtonian simulants were used. Because past 1/4- and 1/2-scale tests used kaolin/ bentonite clay mixtures, clay was used again to compare present and past results. A nonradioactive chemical simulant of pretreated high-level waste (HLW) from Tank 241-AZ-101 (AZ-101) was also chosen, based on the simulant's use in previous small-scale tests and because its chemical composition and rheological properties were similar to those of actual AZ-101 sludge samples [14]. Both clay without AFA and AZ-101 simulant with AFA were tested at nominal yield stresses of 30, 13, and 3 Pa, for a total of six simulant conditions. The yield stress was adjusted by progressively diluting the thicker simulant with water. Simulant rheology was monitored by analyzing samples drawn from the top, central, and bottom regions of the tank before, during, and after each test. Water without AFA and water with increasing concentrations of AFA were also used in initial visualization tests of the qualitative effect of AFA on bubble behavior.

The AFA was added to the AZ-101 simulant at the WTP design basis concentration of 350 mg/L. AFA was not added to the clay because previous tests had shown that a large fraction absorbed on clay solids [8]. At the same time, no tests were performed in AZ-101 simulant without AFA because AFA was needed to prevent surface foaming. Comparing gas holdup tests in AZ-101 simulant with AFA to those in clay without AFA thus shows the combined effects of different simulants and the presence of AFA. The effect of AFA alone could not be distinguished. Data from the small-scale agitator-mixed stand [6] indicated that the effect of AFA alone was less than that seen by comparing AZ-10l simulant with AFA to clay without AFA, but these non-prototypic data may not apply to conditions in the hybrid system.

The total gas volume fraction in the simulant was calculated primarily from the hydrostatic pressure difference between two sensitive pressure transducers at fixed elevations in the simulant. An alternative calculation from changes in the simulant surface level measured with 4 laser range finders was also used for confirmation and backup. This analysis was complicated by the cyclic nature of PJM operation. The fluid level inside and outside the pulse tubes and the slurry velocity and pressure field fluctuate continuously over the 54-second drive cycle. However, the data of interest are differences in level and hydrostatic pressure over tens or hundreds of cycles that are smaller than the variations occurring during a cycle. This difficulty is resolved by using the quiet equilibrium period of ~16 seconds at the end of each cycle, over which measurements recorded at 1 Hz can be aggregated to resolve the small differences between cycles. The gas volume fraction per PJM cycle that is computed from the aggregated 1-Hz data shows the increases and decreases in total gas volume fraction from a starting baseline value during each test. The total gas fraction includes contributions from both in situ-generated gas ("retained gas") and sparger gas holdup.

The total gas volume fraction is calculated from the difference, ΔP, between two hydrostatic pressure measurements separated by a known elevation, ΔH, using

$$\alpha(t) = 1 - \frac{\Delta P(t)}{g\rho_{sim}(t)\Delta H} \qquad \text{(Eq. 8)}$$

where
    ρ_{sim} = bulk, gas-free density of the simulant (kg/m^3)
    ΔH = fixed distance between pressure sensors (m)
    g   = acceleration of gravity (9.81 m/s^2)
    ΔP = pressure difference between the two sensors (Pa).

Setting t = 0, solving Eq. (8) for gΔH, and back-substituting gives

$$\alpha(t) = 1 - \frac{\Delta P(t)}{\Delta P(0)} \frac{\rho_{sim}(0)}{\rho_{sim}(t)}$$ (Eq. 9)

The density, $\rho_{sim}(t)$, is related to $\rho_{sim}(0)$ and the net gain in water mass from the balance of hydrogen peroxide decomposition and evaporation, $\Delta_w(t)$, by

$$\rho_{sim}(t) = \frac{\rho_{sim}(0)V_{sim}(0) + \Delta_w(t)}{V_{sim}(0) + \dfrac{\Delta_w(t)}{\rho_w}}$$ (Eq. 10)

where ρ_w is the density of water at the current simulant temperature. The water mass added with the hydrogen peroxide solution is calculated directly from the injection flow rate assuming complete decomposition. The total water loss due to evaporation is estimated by assuming that the sparge air flow enters the simulant dry and leaves saturated with water vapor at the current simulant temperature. This overestimates the sparge air flow contribution but does not include evaporation from the simulant surface or from the inside of the pulse tubes. Comparison of the density computed from Eq. (10) with sample analysis results indicate that these assumptions provide a reasonable estimate. A gas fraction for sparger holdup alone, based on measurements taken before any H_2O_2 was added, is then subtracted to give the fraction of retained gas alone.

Results from these tests allow determination of a relationship between the steady-state retained gas volume fraction and the gas generation rate (as expressed by the superficial velocity). There are two basic criteria for determining which data represent a satisfactory steady state: the gas volume fraction must be changing in time less than some small rate criterion, and the aggregated steady-state gas volume fraction must be statistically different from the baseline (initial "zero" value). The measure of "steadiness" is the slope obtained from a linear regression on the computed gas volume fractions over the last 30 cycles (excluding the first hour of each 2-hour test segment). A steady state is considered to be present when the absolute value of the slope is less than the specified limit. If this criterion is met, the steady state gas volume fraction is computed as the mean of the 30 values evaluated. If this mean value also satisfies a T-test for significance, it is considered an acceptable steady state.

RESULTS OF TESTING

Water Visualization Tests

The purpose of the water visualization tests was to use visual observations to qualitatively understand the changes in bubble size and dynamics caused by adding AFA. Bubble behavior was recorded by high-speed video at AFA concentrations of 0, 10, 30, 100, and 350 mg/L. Because the surface tension decreases most rapidly from 0 to ~4 mg/L, the visual effect of AFA on bubble behavior was most dramatic at the 10 mg/L concentration.

With PJMs and spargers, the effect of AFA appeared to be mainly a dramatic increase in the number of very small bubbles. An apparent haze was actually tiny bubbles estimated to be less than 100 μm in diameter. However, the behavior (e.g., size, formation frequency, breakup, and coalescence) of the largest bubbles and bubble swarms appeared to be little affected by AFA. In addition, the volume occupied by the increased population of the smallest bubbles was quite low. The sparger holdup remained essentially constant at 1.6 ± 0.8 vol% at all AFA concentrations.

Bubble behavior was extremely complex and can be studied effectively only by viewing the high-speed video in slow motion. The sparge bubbles interacted intensely in low-viscosity water and never assumed the classic Taylor cap shape expected in large bubbles. Bubbles were created at a relatively high rate and small separation distance that produced continually evolving swarms [15]. Individual bubbles accelerated in a loose column, quickly overtaking the leader. At this point the swarm spread out in a mushroom shape and quickly decelerated, only to gather again and accelerate behind the next large rising bubble. One or more bubbles overtaking others caused both coalescence and breakup, often nearly simultaneously. Even at the smallest concentration tested, 10 mg/L, AFA appeared to increase the number of small bubbles created. Though the sparger tube tips are near the PJM nozzle outlet, the PJM jet seemed only to cause a large-scale circulation of smaller bubbles in the lower portion of the tank. The additional turbulence of the jet did not appear to cause additional bubble breakup; whatever breakup occurred was due to bubble interaction in the sparger ROB.

Steady-State Gas Holdup in Clay Simulant Without AFA

The purpose of the clay tests was to confirm that the current test stand, with PJMs and spargers on, could reproduce the baseline gas holdup results of prior clay tests at 30-Pa yield stress, determine the effect of decreasing simulant yield stress on gas holdup, and provide a baseline to compare with the results of tests in AZ-101 simulant. Gas holdup data from current and past tests in clay at about 30 Pa is plotted as a function of superficial velocity in Figure 3. Each data point for the present tests is the mean of a number of per-cycle holdup measurements, and the error bars represent ±1 standard deviation of that mean.

Data from past and current test series, which include both 1/2- and 1/4-scale and a variety of test conditions and operating modes, correspond with each other well. The relative simulant depth varied from 0.74 to 0.93, PJM nozzle velocity from 10 to 17 m/s, and stroke from 50 to 90%. Two of the four data points for the 2004 tests used up-angle nozzles on every other pulse tube with four spargers, while the other two data points used down-angle PJM nozzles and a recirculation loop instead of spargers. Within these limits, gas holdup is apparently not sensitive to the system configuration or operating conditions. Given its consistency over two scales and several configurations, the curve fit line in Figure 4 represents the scaling basis for the WTP lag storage vessel with 30-Pa clay without AFA.
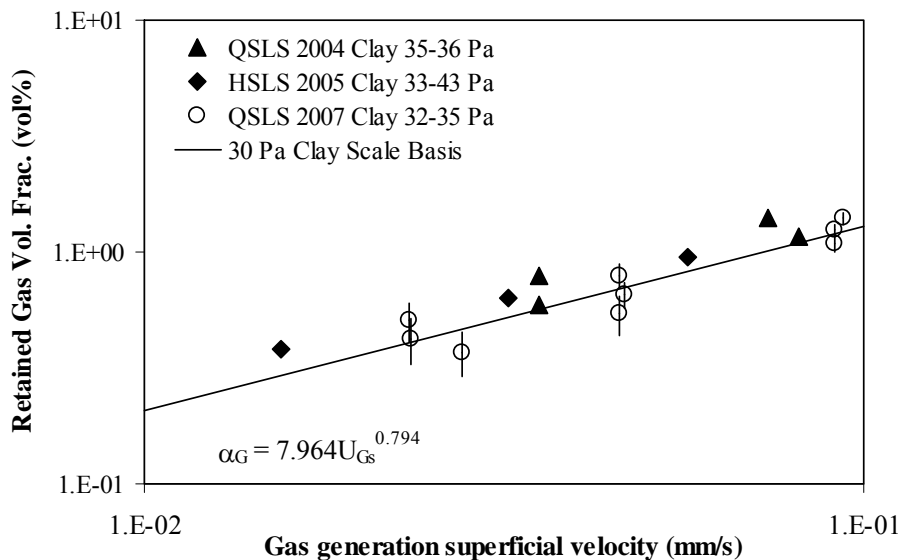

Fig. 3. 30-Pa clay gas holdup scaling basis
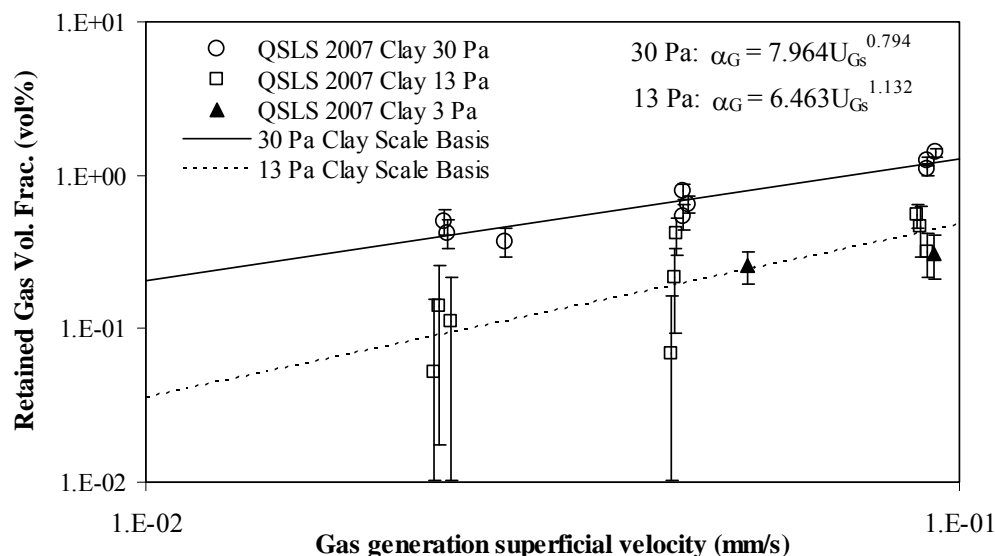**(QSLS = 1/4-scale lag storage; HSLS = 1/2-scale lag storage).**

Fig. 4. Summary of 1/4-scale lag storage clay retained gas holdup data.

Retained gas holdup results from current tests in 30-, 13-, and 3-Pa clay simulant without AFA are compared in Figure 4. The curve-fit scaling bases for both 30-Pa and 13-Pa clay are shown. Gas holdup decreases with decreasing simulant yield stress. The gas holdup at 13 Pa follows about the same trend and is about half that in the 30-Pa clay at 0.1 mm/s. The ratio widens with decreasing superficial velocity. At 0.01 mm/s the holdup at 13 Pa is less than 1/5 that at 30 Pa. The retained gas holdup in the 3-Pa tests was difficult to detect, hence the small number of data points. It would be appropriate to state that the gas holdup in 3-Pa clay without AFA was barely detectable and certainly no greater than that at 13 Pa.

Steady-State Gas Holdup in AZ-101 Simulant with AFA

The tests in AZ-101 simulant containing AFA were conducted to determine whether retained gas holdup was increased as strongly under these conditions, compared to clay without AFA, as had been observed in the earlier tests in the small agitator-mixed vessel at SRNL. The current data show a lesser increase when the prototypic mixing system is used.

Steady-state gas holdup in AZ-101 simulant with AFA at 30-, 13-, and 3-Pa yield stress is shown in Figure 5. The curve-fit scaling bases for 30-Pa and 13-Pa AZ-101 simulant are included. Comparison with Figure 4 shows that at 30 Pa the ratio of holdup in AZ-101 simulant with AFA to that in clay without AFA is higher, approximately 2, than it is at 13 Pa, approximately 1.5. The higher scatter in the 3-Pa data results from an unexplained variability in the sparge gas fraction, which was about 9 vol% in 3-Pa AZ-101 simulant with AFA. Because the retained gas fraction is calculated by subtracting the sparge gas fraction measured at the beginning of the run from the total gas fraction measured at any point in the run, an error in retained gas fraction can result when sparge gas fraction is large and departs from the initial value. Only the 3-Pa AZ-101 simulant with AFA displayed a sparge gas fraction of more than 1 vol%, or showed any variability in the sparge holdup. It is safe to say that the 3-Pa holdup may be as high as in the 13-Pa simulant, but is no higher than the 30-Pa data for the same simulant.
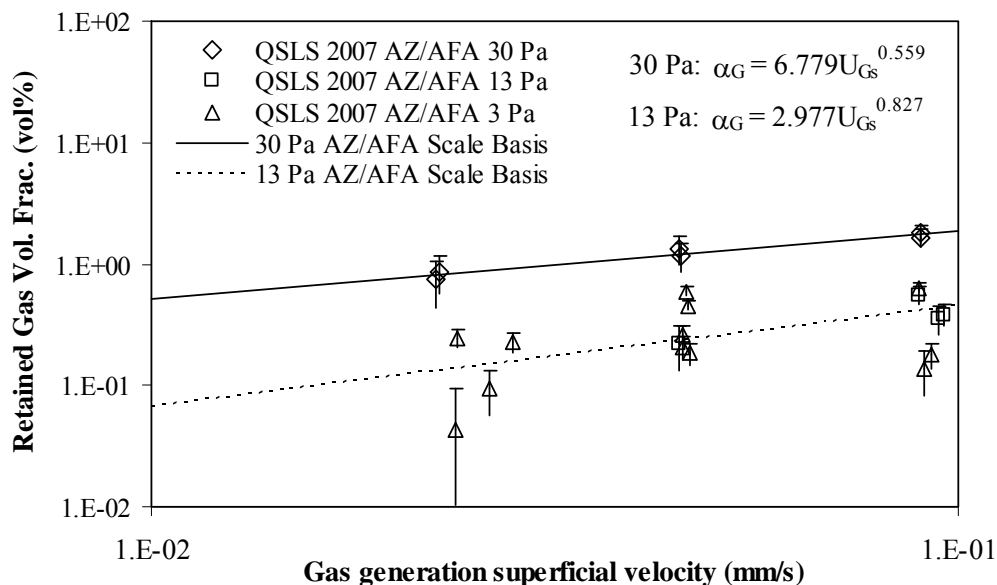
30 Pa: $\alpha_G = 6.779 U_{Gs}^{0.559}$

13 Pa: $\alpha_G = 2.977 U_{Gs}^{0.827}$

Fig. 5. Summary of AZ-101 HLW simulant retained gas holdup data.

Figure 6 compares current retained gas holdup data in 13-Pa simulants to that measured in the SRNL small mixing vessel [6]. Here the holdup measured in 13-Pa clay and AZ-101 simulant with AFA during current tests is similar and matches the SRNL 13-Pa clay data (though these show a different trend with superficial velocity); but the holdup from the SRNL tests in 13-Pa AZ simulant containing AFA are 7 to 10 times as high. This comparison, indicating a higher gas holdup in simulants with lower yield stress, was the primary driver for conducting the current test program.
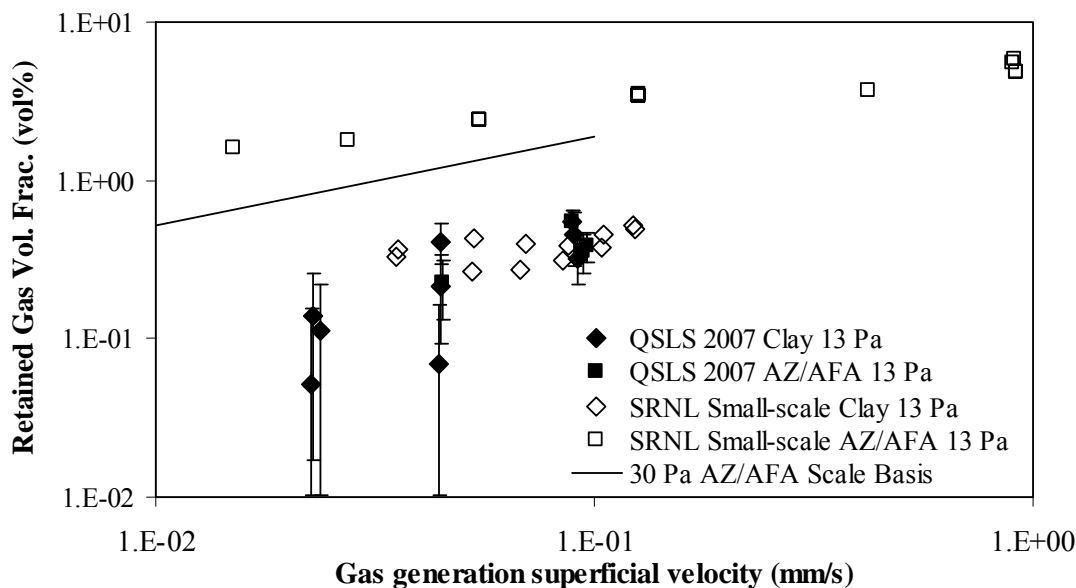

Fig. 6. Comparison of retained gas holdup in 13-Pa clay and AZ-101 HLW simulant.

The primary cause of the difference between the new results and those of the 2006 tests in the SRNL small mixing vessel appears to be the fundamental difference in the cause-and-effect relationship of the bubble size distribution to the mixing system. Any process that enhances breakup or reduces coalescence creates smaller bubbles that rise more slowly and increase gas holdup. The radial agitator in the SRNL vessel was designed specifically to break up larger bubbles that were introduced below it through small tubes [6]. Thus, this system creates the bubble size distribution by the intense turbulence around the agitator blades. The turbulence intensity causing breakup depends on the agitator speed and the density and viscosity (or rheology) of the fluid. The bubble size resulting from breakup events depends on the surface tension of the fluid and whether surfactants or other contaminants are present that affect interface mobility [16]. This mixing system thus amplifies the effects of AFA, which reduces the surface tension, and of reduced yield stress, which increases the intensity of turbulence while decreasing its scale. Both effects tend to create smaller bubbles and thus greater gas holdup, which is consistent with data from the SRNL small agitator-mixed vessel [6].

In the prototypic mixing system using PJMs and spargers, the gas bubbles of interest are nucleated out of the liquid onto small particles and grow by diffusion of dissolved gases and occasional coalescence. As they grow larger, their increasing buoyancy increases their vertical relative velocity with respect to the slurry, and they eventually escape through the surface. During their residence in the slurry they may be carried near the PJM jets, where the largest might break up in the turbulence, and the smaller ones remain unaffected. Except for a few being captured, small bubbles are not likely to be affected by the rising column of large sparge bubbles. This process creates a bubble size distribution that depends mainly on the balance of nucleation, growth, and release and very little on turbulent breakup and bubble interaction. Accordingly, the surface tension, interface phenomena, and simulant yield stress have little direct effect on the size of bubbles produced by gas generation. Yield stress does affect the rise speed of these bubbles, but with the normal trend, higher yield stress slows the rise speed and increases holdup, which is consistent with the current results.

Gas Release Test Results

The gas release tests first allow gas to build up in the simulant while mixing is turned off, then produce a release transient by turning the PJMs and spargers on. Data analysis is based on the assumption that the superficial velocity of gas rising through the simulant during the transient is related to the bulk gas volume fraction by a power function of the same form, $\alpha = AU_S^B$, that expresses the trend of gas holdup tests [6]. With no gas generation, the rate of change of the holdup during a release is expressed in terms of the gas volume fraction and the speed at which bubbles leave the simulant surface, U_R, by

$$\frac{d\alpha}{dt} = \frac{-\alpha U_R}{H} \qquad \text{(Eq. 11)}$$

Substituting Eq. (4) for U_R yields

$$\frac{d\alpha}{dt} = \frac{-1}{H}\left(\frac{\alpha}{A}\right)^{1/B} \qquad \text{(Eq. 12)}$$

For $\alpha(0) = \alpha_0$, Eq. (12) has the solution:

$$\alpha(t) = \left[\alpha_0^{\frac{B-1}{B}} - \left(\frac{B-1}{B} \right) \frac{t}{HA^{1/B}} \right]^{\frac{B}{B-1}}$$

(Eq. 13)

Though the form $\alpha = AU_S^B$ and Eq. (13) consistently provides a good fit to most gas release data [6], the resulting coefficient and exponent generally differ significantly from those expressing the gas holdup versus superficial velocity trend for the same simulant and test stand. Typically, the actual release is slower than described by the holdup parameters. This finding also applies to the current data, although the holdup-derived parameters express the release more closely.

As shown in Figure 7, the 13-Pa clay releases gas somewhat more quickly than 30-Pa clay, but both simulants release essentially all the retained gas in less than 10 minutes. Eq. (13) indicates that the time for release scales linearly with simulant depth. Therefore, a similarly complete release in the full-scale lag storage vessel would occur in less than ~40 minutes. The curve fits for holdup in 30-Pa clay simulant shown in Figure 3 are similar to the power fits listed in Figure 7.

The generated gas release transients in AZ-101 simulant with AFA plotted in Figure 8 are similar to those in clay. If anything, gas release is somewhat faster than in clay. However, the fits derived from Eq. (13) are different from those expressing the steady state holdup given in Figure 5. The holdup parameters for 13 Pa AZ simulant predict a faster release than the data, and those from holdup tests in the 30 Pa AZ simulant show a slower release.
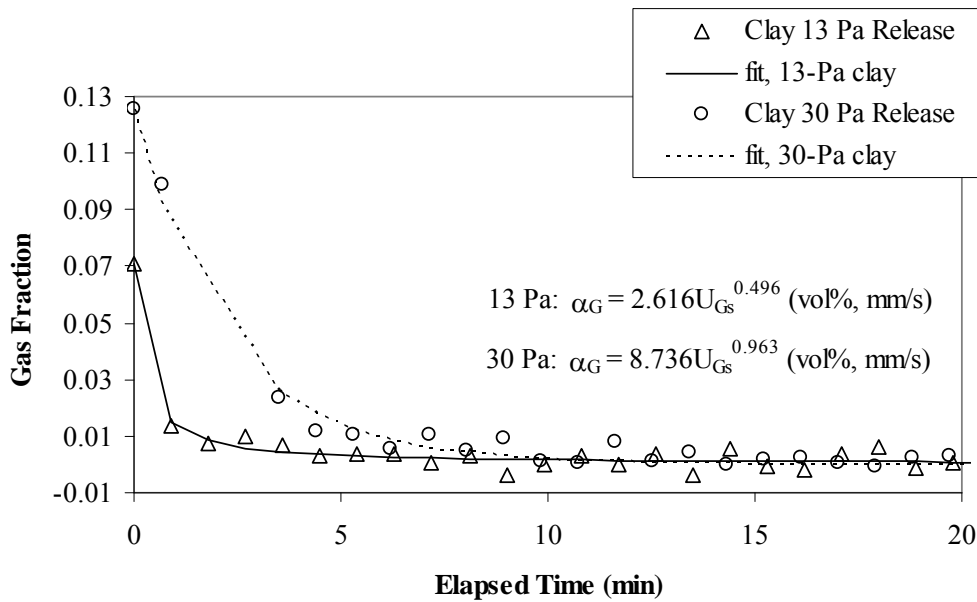

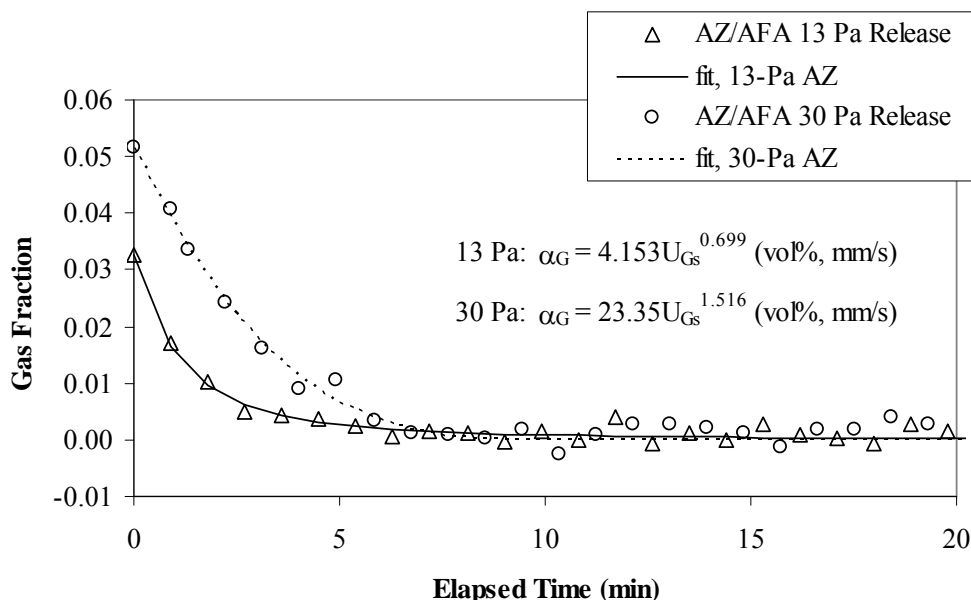Fig. 7. Gas release transients in clay simulant.

Fig. 8. Gas release transients in the AZ-101 HLW simulant.

CONCLUSIONS

The primary conclusions based on the results of the gas retention and release tests in the 1/4-scale test stand are as follows:

- Retention or holdup of gas generated in situ in AZ-101 simulant with AFA was found to be similar to that observed in clay simulant without AFA at a yield stress of 13 Pa and roughly double that in clay with 30 Pa yield stress. This indicates that gas holdup is not as greatly enhanced in chemical simulant containing AFA in a large-scale prototypic mixing system as had been suggested by data from small-scale impeller-mixed systems, which showed factors of up to 10.

- Steady-state gas holdup decreases with decreasing yield stress based on the results of tests in 30-Pa and 13-Pa yield stress simulants. The data for 3-Pa AZ-101 simulant with AFA may have shown gas holdup roughly equal to that in the 13-Pa AZ-101 simulant with AFA, but the results were inconclusive because of interference by large and variable sparger holdup.

- Release of retained gas was relatively rapid and complete in both clay and in AZ-101 simulant with AFA at both 30- and 13-Pa yield stress.

REFERENCES

1. A.P. POLOSKI, P.A. MEYER, L.K. JAGODA, and P.R. HRMA, "Non-Newtonian Slurry Simulant Development and Selection for Pulse Jet Mixer Testing," PNNL-3495, Battelle – Pacific Northwest Division, Richland, Washington (2004).
2. L.M. STOCK, "The Chemistry of Flammable Gas Generation," RPP-6664 Rev. 0, CH2M HILL Hanford Group, Inc., Richland, Washington (2000).
3. P.A. MEYER, D.E. KURATH, and C.W. STEWART, "Overview of the Pulse Jet Mixer Non-Newtonian Scaled Testing Program," PNWD-3677, Battelle – Pacific Northwest Division, Richland, Washington (2005).

4. J.A. BAMBERGER, P.A. MEYER, J.R. BONTHA, C.W. ENDERLIN, D.A. WILSON, A.P. POLOSKI, J.A. FORT, S.T. YOKUDA, H.D. SMITH, F. NIGL, M. FRIEDRICH, D.E. KURATH, G.L. SMITH, J.M. BATES, and M.A. GERBER, "Technical Basis for Testing Scaled Pulse Jet Mixing Systems for Non-Newtonian Slurries," PNWD-3551, Battelle – Pacific Northwest Division, Richland, Washington (2005).

5. A.P. POLOSKI, S.T. ARM, J.A. BAMBERGER, B. BARNETT, R. BROWN, B.J. COOK, C.W. ENDERLIN, M.S. FOUNTAIN, M. FRIEDRICH, B.G. FRITZ, R.P. MUELLER, F. NIGL, Y. ONISHI, L.A. SCHIENBEIN, L.A. SNOW, S. TZEMOS, M. WHITE, and J.A. VUCELICK, "Technical Basis for Scaling of Air Sparging Systems for Mixing in Non-Newtonian Slurries," PNNL-3541, Battelle – Pacific Northwest Division, Richland, Washington (2005).

6. C.W. STEWART, P.A. MEYER, M.S. FOUNTAIN, C.E. GUZMAN-LEONG, S.A. HARTLEY-MCBRIDE, J.L. HUCKABY and B.E. WELLS, "Effect of Anti-Foam Agent on Gas Retention and Release Behavior in Simulated High Level Waste," PNWD-3786, Battelle – Pacific Northwest Division, Richland, Washington (2006).

7. C.W. STEWART, M.E. BREWSTER, P.A. GAUGLITZ, L.A. MAHONEY, P.A. MEYER, K.P. RECKNAGLE, and H.C. REID, "Gas Retention and Release Behavior in Hanford Single-Shell Waste Tanks," PNNL 11391, Pacific Northwest National Laboratory, Richland, Washington (1996).

8. R.L. RUSSELL, S.D. RASSAT, S.T. ARM, M.S. FOUNTAIN, B.K. HATCHELL, C.W. STEWART, C.D. JOHNSON, P.A. MEYER, and C.E. GUZMAN-LEONG, "Final Report: Gas Retention and Release in Hybrid Pulse Jet-Mixed Tanks Containing non-Newtonian Waste Simulants," PNWD-3552, Battelle – Pacific Northwest Division, Richland, Washington (2005).

9. R. CLIFT, J.R. GRACE, and M.E. WEBER, "Bubbles, Drops, and Particles," Academic Press, New York (1978).

10. L.S. FAN and K. TSUCHIYA, "Bubble Wake Dynamics in Liquids and Liquid-Solid Suspensions," Butterworth Heinemann, Stoneham, Massachusetts (1990).

11. A.A. KULKARNI and J.B. JOSHI, "Bubble Formation and Bubble Rise Velocity in Gas-Liquid Systems: A Review," Ind. Eng. Chem. Res., Vol. 44, pp. 5873–5931 (2005).

12. R.P. CHHABRA, "Bubbles, Drops, and Particles in Non-Newtonian Fluids," CRC Press, Boca Raton, Florida (1993).

13. J.R. BONTHA, C.W. STEWART, D.E. KURATH, P.A. MEYER, S.T. ARM, C.E. GUZMAN-LEONG, M.S. FOUNTAIN, M. FRIEDRICH, S.A. HARTLEY, L.K. JAGODA, C.D. JOHNSON, K.S. KOSCHIK, D.L. LESSOR, F. NIGL, R.L. RUSSELL, G.L. SMITH, W. YANTASEE, and S.T. YOKUDA, "Technical Basis for Predicting Mixing and Flammable Gas Behavior in the Ultrafiltration Feed Process and High-Level Waste Lag Storage Vessels with Non-Newtonian Slurries," PNWD-3676, Battelle – Pacific Northwest Division, Richland, Washington (2005.).

14. R.E. EIBLING, R.F. SCHUMACHER, and E.K. HANSEN, "Development of Simulants to Support Mixing Tests for High Level Waste and Low Activity Waste," SRT-RPP-2003-00098 Rev. 0, Westinghouse Savannah River Company, Aiken, South Carolina (2003).

15. C.W. STEWART, "Bubble Interaction in Low-Viscosity Liquids," International J. of Multiphase Flow," Vol. 21, pp. 1037–1046 (1995).

16. R.A. GRAU, "An Investigation of the Effect of Physical and Chemical Variables on Bubble Generation and Coalescence in Laboratory Scale Flotation Cells," TKK-ME-DT-4, Doctoral dissertation, Helsinki University of Technology, Finland (2005).